CHEMISTRY
AN ASIAN JOURNAL

DOI: 10.1002/asia.201100769

Synthesis and Characterization of Two Formyl 2-Tetrazenes

Henri Delalu and Carlos Miró Sabaté*[a]

Abstract: The synthesis of two formyl 2-tetrazenes, namely, (*E*)-1-formyl-1,4,4-trimethyl-2-tetrazene (**2**) and (*E*)-1,4-diformyl-1,4-dimethyl-2-tetrazene (**3**), by oxidation of (*E*)-1,1,4,4-tetramethyl-2-tetrazene (**1**) using potassium permanganate in acetone solution is presented. Compound **3** was also synthesized in an improved yield from the oxidation of 1-formyl-1-methylhydrazine (**4a**) using potassium permanganate in acetone. Both compounds **2** and **3** were characterized by analytical (elemental analysis, GC-MS) and spectroscopic methods (^{1}H, ^{13}C, and ^{15}N NMR spectroscopy, and IR and Raman spectroscopy). In addition, the solid-state structures of the compounds were confirmed by low-temperature X-ray analysis. (Compound **2**: triclinic; space group $P\text{-}1$; $a=5.997(1)$ Å, $b=8.714(1)$ Å, $c=13.830(2)$ Å; $\alpha=107.35(1)°$, $\beta=90.53(1)°$, $\gamma=103.33(1)°$; $V_{UC}=668.9(2)$ Å^3; $Z=4$; $\rho_{calc}=1.292$ cm^{-3}. Compound **3**: monoclinic; space group $P2_1/c$; $a=5.840(2)$ Å, $b=7.414(3)$ Å, $c=8.061(2)$ Å; $\beta=100.75(3)°$; $V_{UC}=342(2)$ Å^3; $Z=2$; $\rho_{calc}=1.396$ g cm^{-3}.) The vibrational frequencies of compounds **2** and **3** were calculated using the B3LYP method with a 6-311+G(d,p) basis set. We also computed the natural bond orbital (NBO) charges using the rMP2/aug-cc-pVDZ method and the heats of formation were determined on the basis of their electronic energies. Furthermore, the thermal stabilities of these compounds, as well as their sensitivity towards classical stimuli, were also assessed by differential scanning calorimetry and standard BAM tests, respectively. Lastly, the attempted synthesis of (*E*)-1,2,3,4-tetraformyl-2-tetrazene (**6**) is also discussed.

Keywords: 2-tetrazenes · hydrazines · NMR spectroscopy · quantum chemistry · X-ray diffraction

Introduction

The study of compounds containing nitrogen-catenated and highly energetic materials for possible energetic application has been the main focus of our research over the last few years.[1–2] Compounds containing catenated N–N bonds are very attractive for use in energetic applications. This attraction is due to the high average two-electron bond energy associated with the N≡N triple bond, which is a unique feature of these compounds and accounts for their high energy content.

At present, a lot of attention is focused on azole chemistry. In particular, triazole- and tetrazole-based energetic materials have been the center of attention.[1–4] This focus is due to the unique properties of these types of compounds. On one side, they are highly energetic (owing to the nitrogen catenation) and, on the other, they are relatively chemically and thermally stable (owing to their aromaticity).

In addition to cyclic energetic materials, open-chain compounds containing catenated nitrogen atoms have also been reported to have interesting energetic properties. For example, Shreeve and co-workers,[5] and later ourselves,[6] reported salts based on the 2,2-dimethyltriazanium cation. The Klapötke group recently reported the synthesis of functionalized 2-tetrazenes.[7–9] These latter compounds have high thermal stabilities and low temperatures of explosion, along with respectable detonation parameters. These interesting energetic properties attracted our attention and prompted us to consider 2-tetrazenes as attractive candidates for energetic applications.

2-Tetrazenes can be generated by oxidation of the corresponding hydrazine (Scheme 1a)[10] and X-ray crystallographic analysis should allow to unequivocally identify the geometry of the double bond. The simplest 2-tetrazene is $H_2N–N=N–NH_2$, which was synthesized by Wiberg et al. from the trimethylsilyl derivative $(Me_3Si)_2N–N=N–N(SiMe_3)_2$ by reaction with trifluoroacetic acid at −78 °C. The overall synthesis started with the silylation of hydrazine to form $(Me_3Si)_2N–NH(SiMe_3)$, which was oxidized into $Me_3Si–N=N–SiMe_3$; final dimerization using SiF_4 afforded $(Me_3Si)_2N–N=N–N(SiMe_3)_2$ (Scheme 1b).[11] Unfortunately, $H_2N–N=N–NH_2$ is thermally labile and decomposes explosively even when stored at 0 °C. Small alkyl chains are known to stabilize thermally labile materials;[12] however, the dimethyl derivative MeHN–N=N–NHMe still remains an elusive species.[13] On the other hand, the tetramethyl de-

[a] Dr. H. Delalu, Dr. C. M. Sabaté
Laboratoire Hydrazines et Composés Ènergétiques Polyazotés,
Université Claude Bernard Lyon 1,
Bât. Berthollet, 22 Av. Gaston Berger, F-69622 Villeurbanne, (France)
Fax: (+33) 472431291
E-mail: carlos.miro-sabate@univ-lyon1.fr

Supporting information for this article is available on the WWW under http://dx.doi.org/10.1002/asia.201100769.

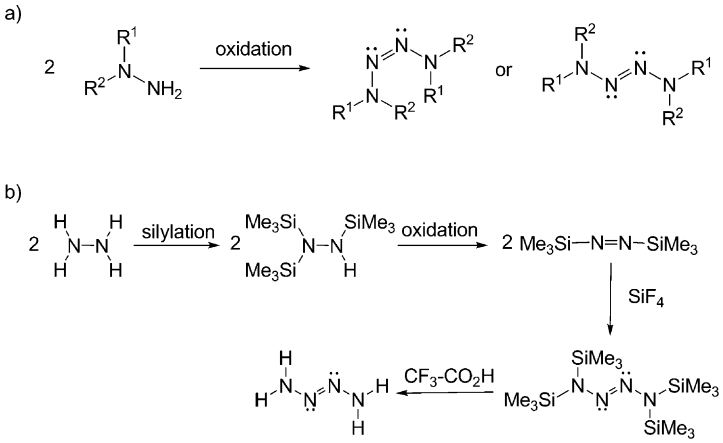

Scheme 1. a) A general procedure for the synthesis of (*Z*)- and (*E*)-2-tetrazenes, and b) the procedure reported by Wiberg et al. for the synthesis of (*E*)-2-tetrazene.

rivative $Me_2N{-}N{=}N{-}NMe_2$ has been reported to be significantly more stable.[14–18]

Herein, we report the synthesis, analytical and spectroscopic characterization, and solid-state crystal structures of two formyl derivatives of $Me_2N{-}N{=}N{-}NMe_2$: (*E*)-1-formyl-1,4,4-trimethyl-2-tetrazene (**2**) and (*E*)-1,4-diformyl-1,4-dimethyl-2-tetrazene (**3**), as well as the attempted synthesis of (*E*)-1,2,3,4-tetraformyl-2-tetrazene (**6**).

Results and Discussion

Synthesis

Oxidation of 1,1-dimethylhydrazine (UDMH) with yellow mercury(II) oxide gave (*E*)-1,1,4,4-tetramethyl-2-tetrazene (**1**)[16] as a pale-yellow liquid (Scheme 2). Although Thun and McBride reported the preparation of compounds **2** and **3**,[19a] these results were difficult to reproduce in our hands and no physical properties or structural characterization of the materials was given. The reaction of compound **1** with one equivalent of potassium permanganate in acetone yielded (*E*)-1-formyl-1,4,4-trimethyl-2-tetrazene (**2**). On the other hand, the reaction of compound **1** with a large excess of potassium permanganate gave (after many attempts) compound **2** as the major product and only a small amount of (*E*)-1,4-diformyl-1,4-dimethyl-2-tetrazene (**3**) was isolated. Furthermore, if compound **2** was isolated and treated with a large excess of potassium permanganate, only a low yield of compound **3** was obtained. Therefore, an alternative procedure for the synthesis of compound **3** was sought and 1-formyl-1-methylhydrazine (**4a**) was synthesized from the formylation of monomethylhydrazine (MMH) with ethyl formate in refluxing ethanol. Subsequently, compound **4a** was oxidized with potassium permanganate to give an improved yield of compound **3**, following a procedure analogous to that reported by Ronco and Erlenmeyer.[20] Hinman and Fulton previously studied the reactions of carboxylic acid esters with methylhydrazine and found that the symmetrical isomer was the predominant product;[21] this work concluded that the yield of the unsymmetrical isomer decreases with increasing size of the acyl group. According to Pedersen,[22] the unsymmetrical isomer should be more favored in the reactions of esters of formic acid owing to both steric and inductive effects. However, regardless of using ethyl formate as the formylating agent, a relatively high yield of the "symmetrical isomer", 1-formyl-2-methylhydrazine (**4b**), was formed (see the Experimental Section).

During our investigation, we did not observe further oxidation of compound **3** to form either the triformyl- (**5**) or tetraformyl derivatives (**6**). Asymmetrically substituted 2-tetrazenes are significantly more-challenging to prepare than their symmetrical analogues. Because compound **3** did not readily oxidize into either compounds **5** or **6**, we decided to attempt the synthesis of the more-readily available tetraformyl derivative (**6**); for this synthesis, we envisaged that 1,1-diformyl hydrazine (**7**) would be a suitable precursor. Unfortunately, following the procedure of Liu et al.[23] for the synthesis of compound **7** by the formylation of aqueous hydrazine with ethyl formate (see Scheme 3) only afforded monoformylhydrazine (**8**) and 1,2-diformylhydrazine (**9**) as the isolated products.

Spectroscopic Discussion

Frequency calculations for compounds **2** and **3** are summarized in the Supporting Information, Tables 1 and 2, together with the experimental IR and Raman spectroscopic data and tentative assignments of the vibration modes. The Gaussian program predicted 51 vibrations for compound **2** and 48 for compound **3** (only selected frequencies are included in the Supporting Information). As might be expected from the structural similarities between both compounds, the vibration modes were also very

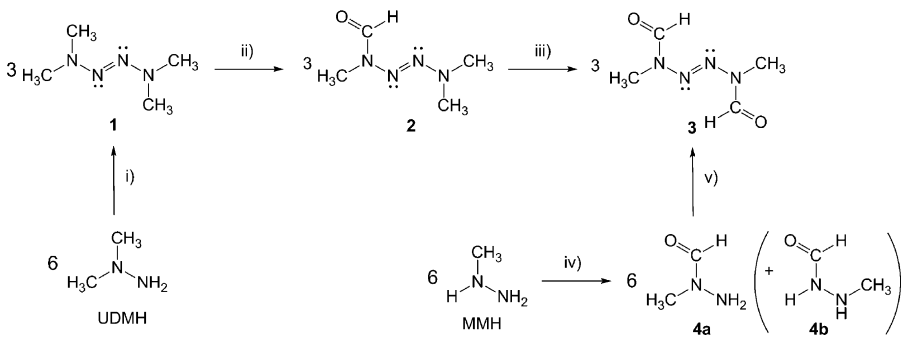

Scheme 2. Synthesis of formyl 2-tetrazenes **2** and **3**: i) HgO (yellow, 6 equiv), 0 °C, Et_2O; ii) $KMnO_4/CaSO_4$ (4 equiv), −70 °C to RT, acetone; iii) $KMnO_4$ (4 equiv), −70 °C to RT, acetone; iv) HCO_2Et (1 equiv), reflux, EtOH; v) $KMnO_4$ (4 equiv), 0 °C to RT, acetone.

CHEMISTRY
AN ASIAN JOURNAL

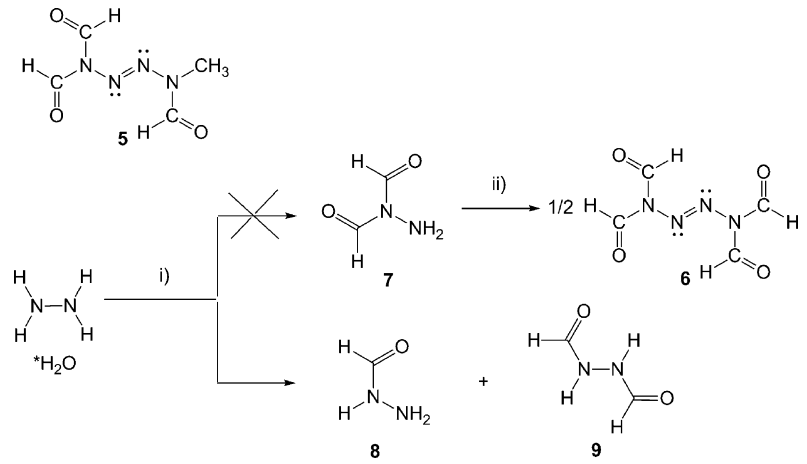

Scheme 3. Attempted synthesis of (*E*)-1,2,3,4-tetraformyl-2-tetrazene (**6**): a) formylation (e.g., HCO_2Et (2 equiv), reflux, EtOH); b) oxidation (e.g., $KMnO_4$ (4/6 equiv), 0 °C to RT, acetone).

similar. Therefore, a joint discussion of the vibration modes for both compounds is useful. In both materials, the two most-important vibrations are the C=O and N=N double-bond stretches. For compound **2**, these stretches were experimentally observed at 1663 cm^{-1} (C=O; by both IR and Raman spectroscopy) and at 1472/1474 and 1443/1429 cm^{-1} (N=N; IR/Raman); for compound **3**, these stretches were observed at 1665/1711 cm^{-1} (C=O; IR/Raman) and 1467/1502 cm^{-1} (N=N; IR/Raman). These wavenumbers were in keeping with the vibrational spectrum of semicarbazidium 5,5′-azobistetrazolate[24] and with the shorter C=O and N=N distances found experimentally for compound **3** than compound **2** (see discussion on the X-ray data). The C–H stretches appeared in the range 2800–3040 cm^{-1} for both materials, with the C4–H stretch having the highest energy. The C–N and N–N stretching modes were at higher energies for compound **3** (1230–1445 cm^{-1}) than compound **2** (1130–1300 cm^{-1}); this observation was in agreement with a higher degree of delocalization in compound **3**, which places more electron density on these bonds. However, the in-plane bending modes of the CH_3 groups appeared experimentally at lower frequencies for compound **3** (1020–1030 cm^{-1}) than compound **2** (1025–1100 cm^{-1}). The same trend applies for the out-of-plane bending modes (**2**: 580–740, **3**: 570–680 cm^{-1}). Below these wavenumbers, torsion and in-plane rocking mode dominated the Raman spectra of the compounds.[25]

The ^1H and ^{13}C NMR spectra of compound **2** showed three resonances in each spectra, whereas the symmetry in derivative **3** accounted for only two signals being observed. In $CDCl_3$, the ^1H NMR resonances of the hydrogen atoms of the methyl groups in compound **2** were very similar: $\delta =$ 3.05 (NMe_2) and 3.19 ppm (N(CHO)Me). However, the aldehyde hydrogen atom appeared at lower field (8.78 ppm). In the ^{13}C NMR spectrum of compound **2** in $CDCl_3$, the resonances of the carbon atoms of the methyl groups were significantly different: $\delta = 27.09$ (N(CHO)Me) and 40.19 ppm (NMe_2), and the aldehyde signal was observed at $\delta =$ 163.23 ppm. The ^1H and ^{13}C NMR shifts observed for the diformyl derivative **3** were very similar to those recorded for the N(CHO)Me part of compound **2**: $\delta = 3.32$ (N(CHO)Me) and 8.94 ppm (CHO) in the ^1H NMR spectrum and $\delta = 27.11$ (N(CHO)Me) and 163.37 ppm (CHO) in the ^{13}C NMR spectrum. Figure 1 shows the ^{15}N NMR spectra of compounds **2** and **3**. The differences between the two compounds were slightly more substantial than in the ^1H and ^{13}C NMR spectra. Whereas the

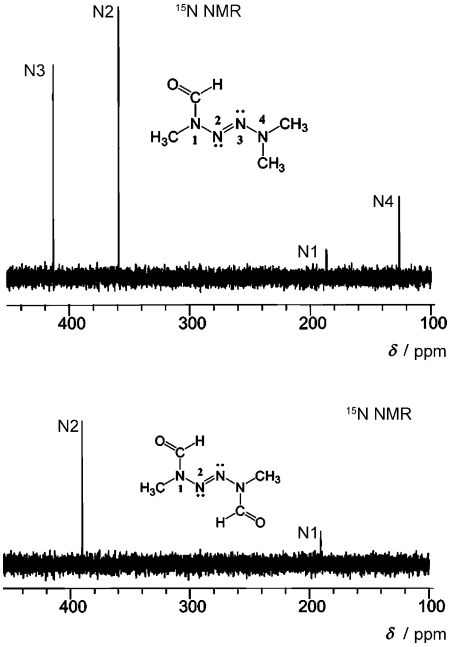

Figure 1. ^{15}N NMR spectra of (*E*)-1-formyl-1,4,4-trimethyl-2-tetrazene (**2**, top) and (*E*)-1,4-diformyl-1,4-dimethyl-2-tetrazene (**3**, bottom) in $CDCl_3$ (NH_3 used as an external reference).

monoformyl derivative (**2**) showed four different resonances for the nitrogen atoms of the azo bridge ($\delta_{N3} = 413.0$ and $\delta_{N2} = 358.8$ ppm), the NMe_2 group ($\delta_{N4} = 125.8$ ppm) and the N(CHO)Me moiety ($\delta_{N1} = 186.2$ ppm); in comparison, compound **3** showed low-field shifts for the resonances of the nitrogen atoms of the azo bridge ($\delta_{N2} = 391.7$ ppm) and of the N(CHO)Me fragment ($\delta_{N1} = 193.2$ ppm).

Lastly, compounds **2** and **3** were also characterized by GC-MS analysis. Compound **2** had a retention time of 22.23 minutes in acetone using method A (17.19 min using method B),[26] whereas compound **3** had a retention time of 23.52 minutes in the same solvent using method C. In the

mass spectrum, the most-intense peak for compound **2** was at $m/z = 130.1$ (100) followed by the mass of the [HN(CH_3)(CHO)] and [CH_2=N(CH_3)] fragments at $m/z = 59.2$ (61) and 43.2 (48), respectively. Other signals with lower intensities included the loss of molecular nitrogen and a [CH_3]$^+$ group at $m/z = 28.2$ (28) and 15.2 (12), respectively, and the loss of [N(CH_3)$_2$]$^+$ and [CHO]$^+$ at $m/z = 86.1$ (7) and 101.2 (3), respectively. As expected, compound **3** showed similar mass fragments: 43.2 (100) [CH_2=N(CH_3)], 144.1 (97) [M]$^+$, 59.2 (31) [HN(CH_3)(CHO)], 48.2 (28) [N_2], 15.2 (21, [CH_3]), and 86.1 (7) [M−N(CH_3)$_2$]$^+$.

X-ray Crystal Structures

For the optimized structures of formyl 2-tetrazenes **2** and **3**, we performed a natural bond orbital (NBO) analysis (Gaussian 03W, see the Supporting Information for a description of the method used). Figures 2 and 3 show the structure of compounds **2** and **3** with their corresponding computed NBO charges. In compound **2**, the nitrogen atoms of the azo bridge (N1 = −0.993e and N6 = −0.345e) and the nitrogen atom of the NMe_2 moiety (N7 = −0.390e) all have negative charges, whereas the nitrogen atom that is closest to the CHO group holds a positive charge (N2 = +0.252e). Similarly, whereas the carbon atoms of the CH_3 groups have similar positive charges (+1.952–+2.006e), the carbon atom of the CHO fragment is less-positively charged (C4 = +1.183e). An analogous situation is found for the diformyl derivative (**3**), where the calculated charges on both sides of the azo bridge are identical by symmetry. In compound **3**, the azo bridge atoms (N1) bear a highly negative charge (−0.829e) whereas the nitrogen atoms of the N(CHO)Me moiety (N2) are positively charged (+0.336e), owing to the CHO fragment pulling electron density away from the nitrogen atoms. In keeping with the electron-withdrawing character of the CHO group, the carbon atom of this latter group (C4) holds a significantly less-positive charge (+1.273e) than that of the carbon atom of the methyl group (C3 = +2.034e). Lastly, the oxygen atoms of both compounds **2** and **3** (O5) have similar highly negative charges (**2**: −0.779e, **3**: −0.750e). It is precisely these oxygen atoms that are involved in the formation of nonclassical C···O hydrogen-bonding interactions (see X-ray analysis below).

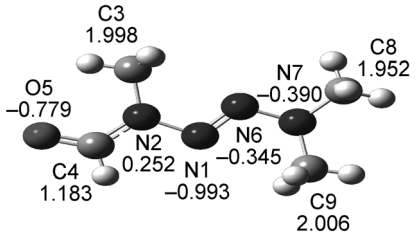

Figure 2. Optimized geometry and charge distribution for (*E*)-1-formyl-1,4,4-trimethyl-2-tetrazene (**2**), as determined by NBO analysis (rMP2/aug-cc-pVDZ).

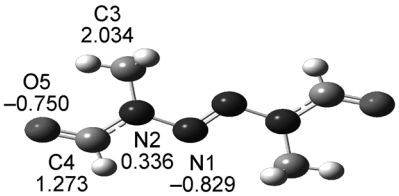

Figure 3. Optimized geometry and charge distribution for (*E*)-1,4-diformyl-1,4-dimethyl-2-tetrazene (**3**), as determined by NBO analysis (rMP2/aug-cc-pVDZ).

The gas-phase geometries of compounds **2** and **3** were calculated using the B3LYP hybrid density functional with the 6-311++G(d,p) basis set.[27] The optimized geometries of the gas-phase structures (B3LYP and MP2) are in very good agreement with the solid-state X-ray diffraction data, as expected for compounds that only present weak interactions in the solid state.

X-ray studies clearly confirmed the *trans* geometry of compounds **2** and **3** (Table 1). Figure 4 shows the two crystallographically independent molecules of compound **2** in the asymmetric unit. The azo-bridge N=N bond distances (1.260(5) and 1.258(5) Å) in compound **2** were slightly

Table 1. Crystal structure solution and refinement of formyl 2-tetrazenes **2** and **3** and of formyl hydrazine **8**.

	2	**3**	**8**
CCDC No.[29]	824059	824058	279587
Formula	$C_4H_{10}N_4O$	$C_4H_8N_4O_2$	CH_4N_2O
M_r	130.15	144.14	60.05
T [K]	293(2)	293(2)	293(2)
description	plate	block	needle
color	colorless	colorless	colorless
crystal size [mm]	0.56×0.21×0.10	0.21×0.15×0.14	0.10×0.03×0.02
crystal system	Triclinic	Monoclinic	Monoclinic
space group	P-1	$P2_1/c$	$P2_1/n$
a [Å]	5.997(1)	5.840(2)	3.737(1)
b [Å]	8.714(1)	7.414(3)	10.609(1)
c [Å]	13.830(2)	8.061(2)	6.574(1)
α [°]	107.35(1)	90	90
β [°]	90.53(1)	100.75(3)	95.11(1)
γ [°]	103.33(1)	90	90
V [Å^3]	668.9(2)	342(2)	259.60(8)
Z	4	2	4
ρ_{calc} [g cm^{-3}]	1.292	1.396	1.537
μ($Mo_{K\alpha}$) [mm^{-1}]	0.815	0.110	1.144
F(000)	280	152	128
θ range [°]	3.35–66.59	3.60–29.20	7.95–65.88
index ranges	$-7 \le h \le 7$	$-7 \le h \le 7$	$-4 \le h \le 4$
	$-10 \le k \le 10$	$-9 \le k \le 9$	$-12 \le k \le 11$
	$-16 \le l \le 15$	$-10 \le l \le 10$	$-6 \le l \le 7$
total reflns	4909	4763	842
unique reflns	2315	853	454
R_{int}	0.056	0.021	0.044
data/restraints/parameters	2315/0/164	853/0/46	454/0/38
R(F)/wR(F^2) (all reflns)[a]	0.0979/0.1887	0.0377/0.0413	0.0606/0.1786
GOF on F^2[a]	1.014	1.050	1.042
$\Delta\rho_{fin}$ (max/min) [e Å^{-3}]	−0.41/0.58	−0.15/0.20	−0.38/0.28

[a] $R_1 = \Sigma\,||F_o| - |F_c||/\Sigma|F_o|$; $R_w = [\Sigma(F_o^2 - F_c^2)/\Sigma w(F_o)^2]^{1/2}$; $w = [\sigma_c^2(F_o^2) + (xP)^2 + yP]^{-1}$, $P = (F_o^2 + 2F_c^2)/3$.

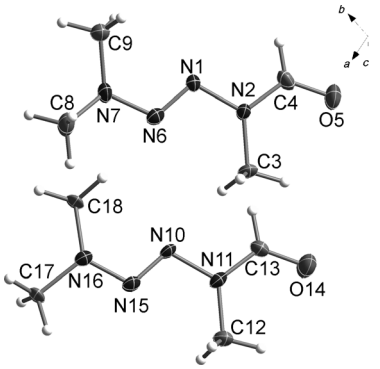

Figure 4. View of the asymmetric unit of compound **2** (ellipsoids set at 60% probability).

longer than the analogous distances in compound **3**; these values fitted well with the expected double-bond character of this bond. However, the remaining two N–N distances were shorter (N6–N7 = 1.355(5) Å and N15–N16 = 1.353(5) Å) and significantly longer (N1–N2 = 1.416(5) Å and N10-N11 = 1.409(4) Å) than the corresponding distance in compound **3** (1.377(1) Å). The elongation of these latter N–N bonds might be attributed to conjugation with the formyl group, which, in the case of compound **3**, are mutually cancelled out owing to the symmetry of the molecule. Note that the N2–C4/N11–C13 distances (1.341(5)/1.334(5) Å) for compound **2** were shortened with respect to those of compound **3** (1.358(1) Å), whereas the C4–O5/C13–O14 distances (1.232(5)/1.222(5) Å) in compound **2** were elongated with respect to compound **3** (1.215(1) Å).

In the unit cell, compound **2** formed planar layers that interacted through weak nonclassical hydrogen bonds (C8–$O5^{ii}$ = 3.791(6) Å, symmetry code: (i) $-x$, $-y$, $1-z$), which (using graph-set nomenclature)[28,29] gave R2,4(12) ring networks. The other two nonclassical hydrogen bonds (C9···$O5^{i}$ = 3.477(6) Å and C18···$O14^{i}$ = 3.478(6) Å, symmetry code: (ii) $1+x$, $1+y$, z) connected molecules of compound **2** together to form C1,1(8) infinite chains (Figure 5). Lastly, ring graph-sets of the type R2,2(16) and R4,4(32) were also formed.

In compound **3** (Figure 6), half of the molecule was generated by symmetry (symmetry code: (i) $1-x$, $-y$, $1-z$). The solid-state structure contained one short N–N bond (N1–

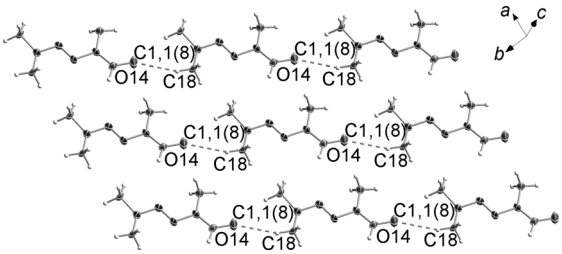

Figure 5. Extended crystal structure of compound **2**, showing intermolecular hydrogen-bonding interactions (dotted lines; C12···$O18^{i}$ = 3.478(6) Å; symmetry code: (i) $1+x$, $1+y$, z) and the C1,1(8) chain networks.

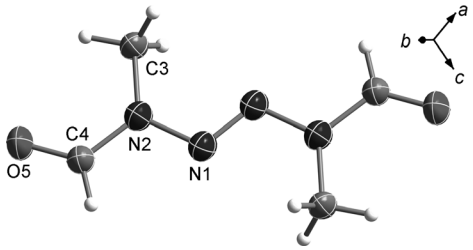

Figure 6. Molecular structure of compound **3** (ellipsoids set at 50% probability).

$N1^{i}$ = 1.247(2) Å), which had clear double-bond character (N=N double bond = 1.245 Å) and one elongated N–N bond (N1–N2 = 1.377(1) Å), which was shorter than the average N–N single-bond distance (1.454 Å)[30] and was indicative of conjugation. This last result was supported by two observations: 1) the shorter N–C bond distance of the N–C(O)H fragment (N2–C4 = 1.358(1) Å) compared to the N–CH_3 fragment (N2–C3 = 1.452(1) Å), and 2) the planarity of the molecule.

Compound **3** was involved in two very directional interactions (C-H-O = 169.0(1)° and 175.2(1)°), between the oxygen atoms of one molecule of compound **3** and the hydrogen atoms of a second molecule. The two nonclassical hydrogen bonds (C4···$O5^{i}$ = 3.474(2) Å and C3···$O5^{ii}$ = 3.590(2) Å; symmetry codes: (i) x, $0.5-y$, $0.5+z$, (ii) $1+x$, y, z) were similar in strength to those found in energetic picrate salts[31] and described different graph-set patterns,[28,29] such as chain motifs of the type C1,1(X) (X = 3, 5, 8), C1,2(X) (X = 6, 9), C2,2(X) (X = 8, 11, 13, 16), and one R2,2(16) ring motif (Figure 7).

As mentioned above, formylation of hydrazine hydrate resulted in the formation of compounds **8** and **9**. The unit cell for compound **9** matches that previously reported.[32] On the other hand, the structure of compound **8** has not been described previously. Compound **8** crystallized in a monoclinic cell in the space group $P2_1/n$.[33] The C1–O1 bond distance (1.238(3) Å) was longer than for a typical C=O double bond and the C1–N1 distance (1.316(3) Å) was shorter than that

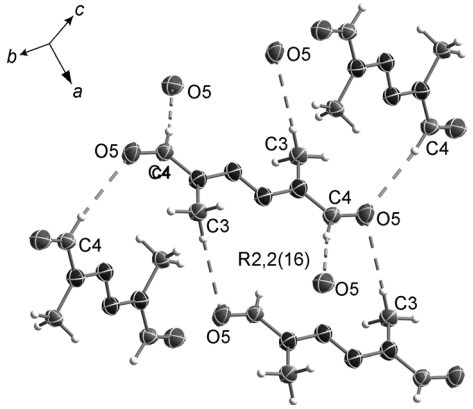

Figure 7. Close packing in the crystal structure of compound **3**, showing hydrogen-bonding interactions (dotted lines) and the formation of a R2,2(16) ring pattern.

of a typical C–N single bond, thereby indicating the amide character of the C(=O)N moiety. On the other hand, the N1–N2 distance of the hydrazine moiety (1.413(3) Å) was shorter than that of $H_2N–NH_2$ (1.449 Å)[34] and slightly elongated compared to the analogous distance in salts based on the 3,4,5-triamino-1,2,4-triazolium cation (ca. 1.400 Å).[35] The three hydrogen bonds in the molecule participate in the formation of four medium-to-strong hydrogen bonds (see Table 2). The hydrogen bond between the N1 atom of one molecule and the O1 atom of another (N1···O1^{iii} = 2.860(3) Å; symmetry code: (iii) $-0.5+x$, $0.5-y$, $0.5+z$) represents the shortest non-covalent interaction in this compound and results in the formation of infinite chains along a direction parallel to the *c* axis.

Compound **8** crystallizes to form layers that are hydrogen-bonded to one another (N2···O1^{i} = 3.114(3) Å; symmetry code: (i) $0.5-x$, $0.5+y$, $0.5-z$). The hydrogen-bonding networks found in the solid state can be better understood by graph-set analysis.[28,29] The Supporting Information, Table 3, contains a summary of the graph-set analysis results. At the primary level, infinite chains of different sizes with the descriptor C1,1(*X*) (*X* = 3–5) are formed. At the secondary level, in addition to infinite chain motifs of the type C1,2(5) and C2,2(*X*) (*X* = 6–9), several R2,1(5), R2,4(X) (*X* = 8, 10), and R4,4(*X*) (*X* = 12, 16, 18, 20) ring networks are also formed (Figure 8). For example, the interaction between the NH and CHO groups of two molecules of compound **8** (N1···O1^{iii} = 2.860(3) Å and N1···N2^{iii} = 3.187(3) Å; symmetry code: (iii) $-0.5+x$, $0.5-y$, $0.5+z$) form R2,1(5) graph-sets and hydrogen bonding of four molecules of compound **8** lead to the formation of R2,4(10) and R4,4(12) motifs. Lastly, a view of a supercell of the compound along the *a*-axis (Figure 9) gives a feeling for the extensive hydrogen bonding present in the structure of the compound, which in combination with a layered structure accounts for the relatively high density of the material (ρ_{calc} = 1.537 g cm^{-3}).

Table 2. Geometries of selected hydrogen bonds in the crystal structures of compounds **2**, **3**, and **8**.

D–H···A[a]	D–H [Å]	H···A [Å]	D···A [Å]	D–H···A [°]
(*E*)-1-formyl-1,4,4-trimethyl-2-tetrazene (**2**)				
C9–H91···O5^{i}	0.950(1)	2.580(2)	3.477(4)	157.2(1)
C18–H181···O14^{i}	0.950(1)	2.570(2)	3.478(5)	160.4(1)
(*E*)-1,4-diformyl-1,4-dimethyl-2-tetrazene (**3**)				
C4–H41···O5^{i}	0.930(1)	2.550(2)	3.473(2)	169.4(1)
monoformylhydrazine (**8**)				
N2–H21···O1^{i}	0.865(1)	2.263(2)	3.114(3)	167.5(1)
N2–H22···O1^{ii}	0.876(2)	2.438(2)	3.175(3)	142.1(1)
N1–H11···O1^{iii}	0.836(1)	2.098(2)	2.860(3)	151.3(1)
N1–H12···N2^{iii}	0.836(1)	2.540(3)	3.187(3)	135.0(1)

[a] Symmetry codes for **2**: (i) 1+x, 1+y, z. **3**: (i) x, 0.5−y, 0.5+z and **8**: (i) 0.5−x, 0.5+y, 0.5−z; (ii) 0.5+x, 0.5−y, 0.5+z; (iii) −0.5+x, 0.5−y, 0.5+z.

Table 3. Selected bond distances [Å] and angles [°] in the crystal structures of compounds **2** and **3**, and comparison with the optimized calculated parameters.[a]

	2 (A)	**2** (B)	B3LYP[b]	MP2[c]	**3**	B3LYP[b]	MP2[c]
N1–N2	1.416(5)	1.409(4)	1.380	1.365	1.377(1)	1.366	1.367
N1–N6[d]	1.260(5)	1.258(5)	1.252	1.282	1.247(1)	1.248	1.279
N2–C3	1.447(5)	1.463(5)	1.456	1.458	1.452(1)	1.458	1.454
N2–C4	1.341(5)	1.334(5)	1.375	1.457	1.358(1)	1.385	1.385
N6–N7	1.353(5)	1.355(5)	1.354	1.378	–	–	–
N7–C8	1.443(5)	1.446(5)	1.456	1.453	–	–	–
N7–C9	1.449(5)	1.463(5)	1.457	1.378	–	–	–
C4–O5	1.232(5)	1.222(5)	1.213	1.230	1.215(1)	1.209	1.226
N1-N2-C3	121.6(3)	121.9(3)	122.5	–	122.5(1)	122.7	122.6
N1-N2-C4	114.5(3)	114.7(3)	115.0	–	114.4(1)	114.8	114.4
N2-N1-N6[d]	110.2(3)	109.9(3)	112.7	111.1	112.0(1)	113.2	111.5
N7-N6-N1	113.2(3)	113.6(3)	114.6	112.9	–	–	–
N2-C4-O5	124.2(4)	125.0(4)	124.6	124.3	123.8(1)	124.1	123.9
C3-N2-C4	123.9(4)	123.4(3)	122.4	122.9	122.8(1)	122.5	123.0
N6-N7-C8	119.3(3)	119.5(3)	119.6	118.0	–	–	–
N6-N7-C9	113.7(3)	113.1(3)	112.6	110.3	–	–	–
C8-N7-C9	119.2(3)	118.6(3)	117.8	115.7	–	–	–

[a] For assignment, see Figures 2 and 3; [b] B3LYP/6-31+G(d,p); [c] MP2/6-31++G-(d,p); [d] N1-N1^{i} and N2-N1-N1^{i} for compound **3** (symmetry code: (i) 1−*x*, −y, 1−*z*).

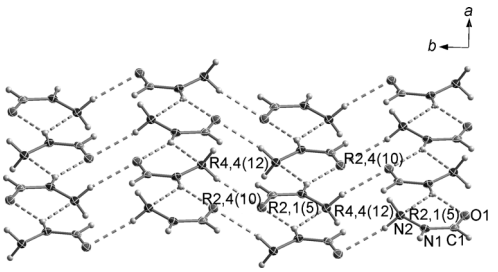

Figure 8. View along the *c* axis in the crystal structure of compound **8**, showing hydrogen-bonding interactions (dotted lines). Selected bond distances (Å) and angles (°): C1–O1 1.238(3), C1–N1 1.316(3), N1–N2 1.413(3); O1-C1-N1 127.3(2), C1-N1-N2 120.8(2).

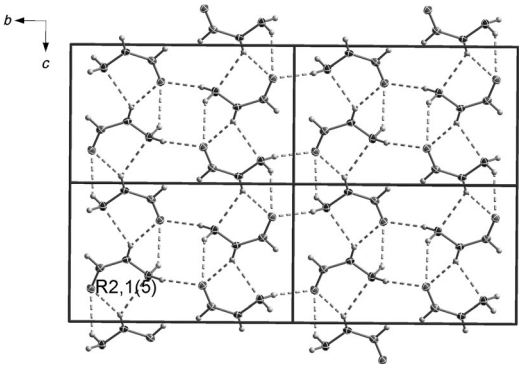

Figure 9. Hydrogen-bonding interactions (dotted lines) in the 2*2*2 [−1−+1] supercell of compound **8** (viewed along the *a* axis).

Physical and Chemical Properties

The thermodynamic data of 2-tetrazenes **2** and **3** (in both the *cis*- and *trans*- forms) were calculated by quantum chemical methods using the computer program Gaussian G03W-B.03. A full explanation of the method used here can be found in the Supporting Information.

Table 4. Enthalpies ($\Delta_f H°$) and energies of formation ($\Delta_f U°$) of compounds **2** and **3** in the solid state.

	$\Delta_f H°$(g) [kcal mol^{-1}]	$\Delta_f H°$(s) [kcal mol^{-1}]	$\Delta_f H°$(s) [kJ mol^{-1}]	Δn[a]	$\Delta_f U°$(s) [kcal mol^{-1}]	M [g mol^{-1}]	$\Delta_f U°$(s) [kJ kg^{-1}]
trans-**2**	+25.6	+10.9	+45.8	−7.5	+15.4	130.15	+495.0
trans-**3**	−10.2	−29.9	−125.1	−7	−25.7	144.13	−747.7
cis-**2**	+40.6	+26.0	+108.7	−7.5	+30.4	130.15	+978.5
cis-**3**	+9.0	−10.5	−44.2	−7	−6.4	144.13	−186.8

[a] Δn = change in the number of moles of gaseous components during the formation of compounds **2** and **3**.

As shown in Table 4, compound **2** is formed endothermically ($\Delta_f H°$(*trans*-**2**) = +45.8 kJ mol^{-1}, $\Delta_f H°$(*cis*-**2**) = +108.7 kJ mol^{-1}) whereas the diformyl derivative (**3**) is formed exothermically ($\Delta_f H°$(*trans*-**3**) = −125.1 kJ mol^{-1}, $\Delta_f H°$(*cis*-**3**) = −44.2 kJ mol^{-1}).

Table 5 contains a summary of some physical and chemical properties of interest for 2-tetrazenes **2** and **3.** The melting points and thermal stabilities (i.e., decomposition points) of both materials were assessed by differential scanning calorimetry (DSC). Both compounds **2** and **3** show distinctive melting points at about 54 °C and about 164 °C for compounds **2** and **3**, respectively (see the Supporting Information, Figures 1 and 2). Note, tetramethyl-2-tetrazene **1** is a pale-yellow liquid with a pungent tetrazene odor that boils at about 130 °C. Both compounds **2** and **3** were obtained as colorless crystalline solids. Compound **2** is thermally stable up to about 182 °C and can easily be purified by sublimation. On the other hand, the higher-melting diformyl derivative (**3**) boils without decomposition at about 195 °C. In the "flame test" (i.e., response to thermal shock) both compounds **2** and **3** burned normally and free of residue.

Table 5. Physical and chemical properties of 2-tetrazenes **2** and **3**.

	trans-**2**	*trans*-**3**
formula	$C_4H_{10}N_4O$	$C_4H_8N_4O_2$
M_r	130.15	144.13
m.p. [°C][a]	54.0	164.0
T_d [°C][b]	182.5	201.4
N [%][c]	43.05	38.87
N+O [%][d]	55.33	61.07
Ω [%][e]	−147.5	−111.0
ρ [g cm^3][f]	1.292	1.396
$\Delta_f U°$ [kJ kg^{-1}][g]	+495	−747
$\Delta_f H°$ [kJ kg^{-1}][h]	+352	−867

[a] Chemical melting point and [b] decomposition point (DSC onsets) from measurement with β = 5 °C min^{-1}; [c] Nitrogen percentage; [d] Combined oxygen and nitrogen content; [e] Oxygen balance; [f] Calculated density (from X-ray measurements); [g] Predicted energy of formation; [h] Predicted enthalpy of formation.

In addition to DSC analysis, we used standard BAM procedures[36–40] to assess the sensitivity of compounds **2** and **3** towards impact and friction. Crystalline samples of both compounds **2** and **3** showed decreased sensitivities towards impact and friction. Compounds **2** and **3** decomposed nonexplosively in the friction tester at 360 N and 324 N, respectively, and in the drop-hammer, nonexplosive decomposition was observed for compound **3** (i = 35 J) whereas compound **2** remained unmodified at i > 40 J. By comparison, these values are significantly lower than those of commonly used TNT or RDX.[41]

Conclusions

Oxidation of 1,1-dimethylhydrazine with yellow mercury(II) oxide gives (*E*)-1,1,4,4-tetramethyl-2-tetrazene (**1**), which can be further oxidized with potassium permanganate to form (*E*)-1-formyl-1,4,4-trimethyl-2-tetrazene (**2**) and (*E*)-1,4-diformyl-1,4-dimethyl-2-tetrazene (**3**) as highly crystalline solids. No further oxidation to form the triformyl- (**5**) or the tetraformyl (**6**) derivatives was observed. Direct oxidation of compound **1** to form compound **3** resulted only in low yields and compound **3** was best synthesized by oxidation of 1-formyl-1-methylhydrazine (**4a**) with potassium permanganate. Hydrazine **4a** was synthesized by formylation of monomethylhydrazine with ethyl formate. Formylation of aqueous hydrazine resulted in the formation of either monoformylhydrazine (**8**) or 1,2-diformylhydrazine (**9**). All compounds in this work were characterized by analytical and spectroscopic methods and the solid-state structures of 2-tetrazenes **2** and **3** and that of formyl hydrazine **8** were determined by low-temperature X-ray crystallography. DSC analysis revealed high chemical and thermal stabilities for compounds **2** and **3** above 180 °C and standard BAM tests showed decreased sensitivities towards impact and friction. The 2-tetrazene derivatives, compounds **2** and **3**, may be potentially useful building blocks for the synthesis of energetic compounds. Preliminary toxicity tests of solid 2-tetrazene derivatives showed lower vapor pressures in comparison to neutral (liquid) hydrazine (e.g., $Me_2N{-}NH_2$) or 2-tetrazene derivatives (e.g., $Me_2N{-}N{=}N{-}NMe_2$), which suggests the potential of compounds **2** and **3** for the synthesis of energetic compounds with lower toxicities.

Experimental Section

Safety Note

2-Tetrazenes and their derivatives are potentially explosive compounds. Although preliminary testing showed low sensitivity of the compounds reported herein towards impact and friction, great care must be taken when operating with 2-tetrazenes, in particular when working on a larger scale. In any case it is recommended that the synthesis of this type of material is to be carried out only by experienced personnel with the best safety practices and whilst wearing protective equipment such as Kevlar gloves, earthed shoes, leather coat, face shield, ear plugs, etc. and using nonconductive equipment.

*Synthesis of (E)-1,1,4,4-Tetramethyl-2-tetrazene (**1**)*

Compound **1** was synthesized according to a literature procedure:[16] 98% 1,1-dimethylhydrazine (89 mL, 1.15 mol) was reacted with yellow mercury oxide (252.20 g, 1.16 mmol) in Et_2O (400 mL) in an ice bath. Sodium carbonate (ca. 20 g) was added in one portion and the reaction mixture was stirred for 1 h in the ice bath and then for 4 h at RT. Next, the insoluble compounds were removed by filtration through Celite and

the filtrate was dried with sodium sulfate. The solvent was then removed under reduced pressure and the bright-yellow crude product was vacuum distilled to give a pale-yellow liquid (90.57 g, 68%). This compound was used in the subsequent oxidation reactions. ^{1}H NMR ($CDCl_3$, 400.18 MHz, TMS): $\delta = 2.73$ ppm (12H, s; CH_3).

*Synthesis of (E)-1-Formyl-1,4,4-trimethyl-2-tetrazene (**2**)*

Compound **2** was synthesized according to a modified literature procedure[19a] as follows: compound **1** (1.16 g, 20.0 mmol) was dissolved in acetone (200 mL) and potassium permanganate (2.12 g, 26.83 mmol) was added portionwise to form a dark-purple solution. Then, calcium sulfate (ca. 3 g) was added in one portion. The dark suspension warmed instantly and manganese(IV) oxide started to precipitate. The reaction mixture was then stirred at room temperature until the solution turned colorless (ca. 1 h) and then more potassium permanganate (2.12 g, 26.83 mmol) was added. The resulting suspension was stirred again until the supernatant liquid became colorless (ca. 1 h) and the solution was then filtered through a plug of Celite. The Celite was then washed with acetone and the combined acetone filtrates were evaporated to dryness (45 °C, 200 mbar), leaving behind a pale-yellow liquid. Slow cooling of the liquid to room temperature resulted in the formation of crystalline compound **3**, which was dried for a short time under high vacuum (0.581 g, 45%). No further purification was necessary. Needlelike single crystals of the compound were grown by letting the concentrated mother liquor stand at room temperature for about 3 days. ^{1}H NMR ($CDCl_3$, 400.18 MHz, TMS): $\delta = 3.05$ (6H, s; CH_3), 3.19 (3H, s; CH_3), 8.78 ppm (1H, s; CHO); ^{13}C{^{1}H} NMR ($CDCl_3$, 100.52 MHz, TMS): $\delta = 27.09$ (1C; N−CH_3), 40.19 (2C, N−CH_3), 163.23 ppm (1C; CHO); ^{15}N NMR ($CDCl_3$, 40.51 MHz, NH_3): $\delta = +413.0$ (1N, s; N3), +358.8 (1N, s; N2), +186.2 (1N, s; N1), +125.8 ppm (1N, s; N4); DSC (5 °C min^{-1}): two endothermic peaks (peak 1: sharp, onset: 54.0 °C, maximum: 56.8 °C; peak 2: broad, onset: 196.2 °C, maximum: 213.6 °C), one exothermic peak (sharp, onset: 182.5 °C, maximum: 186.3 °C); GC: 22.25 (acetone, method A[26]), 17.19 min (acetone, method B[26]); GC-MS (ESI): *m*/*z* (%): 131.1 (7) $[M+H]^+$, 130.1 (100) $[M]^+$, 101.2 (3) $[M-CHO]^+$, 87.1 (15) $[M+H-N(CH_3)_2]^+$, 86.1 (7) $[M-N(CH_3)_2]^+$, 73.1 (6) $[HN{=}NN(CH_3)_2]$, 59.2 (61) $[HN(CH_3)(CHO)]$, 43.2 (48) $[CH_2{=}N(CH_3)]$, 28.2 (28) $[N_2]$, 15.2 (12) $[CH_3]^+$; MS (ESI-ToF, $CHCl_3$/MeOH): *m*/*z* (%): 283.2 (39) $[2M+Na]^+$, 261.2 (41) $[2M+H]^+$, 153.1 (22, $[M+Na]^+$, 131.1 (100) $[M+H]^+$, 130.1 (1) $[M]^+$; Raman (rel. int.): $\tilde{\nu}$ = 3014(47), 2972(23), 2927(26), 2898(27), 2875(18), 2804(10), 1692(4), 1663(73), 1474(100), 1459(27), 1429(94), 1408(14), 1399(12), 1380(15), 1369(30), 1301(11), 1204(43), 1138(12), 1097(3), 1051(2), 1025(25), 904(18), 850(1), 738(2), 584(25), 506(2), 417(10), 386(21), 342(9), 309 cm^{-1} (23); IR (golden gate, rel. int.): $\tilde{\nu}$ = 3032(w), 2972(w), 2944(w), 2893(w), 2890(w), 2801(w), 1749(w), 1663(s), 1472(m), 1443(m), 1409(m), 1400(m), 1385(m), 1368(m), 1298(m), 1227(m) 1204(m), 1140(w), 1093(w), 1052(w), 1027(s), 904(w), 847(m), 738(m), 669(w), 583 cm^{-1} (m); elemental analysis calcd (%) for $C_4H_{10}N_4O$ (130.15): C 36.91, H 7.74, N 43.05; found: C 36.73, H 7.63, N 42.83.

*Synthesis of (E)-1,4-Diformyl-1,4-dimethyl-2-tetrazene (**3**)*

Method 1: Compound **3** was synthesized by the method described above for (*E*)-1-formyl-1,4,4-trimethyl-2-tetrazene (**2**) and using the following amounts of reagents: compound **1** (2.32 g, 20.0 mmol), acetone (200 mL), potassium permanganate (8.48 g, 53.66 mmol). No calcium sulfate was added and the reaction time was about 19 h. Prism-shaped single crystals of the title compound crystallized out of the concentrated mother liquor on standing for about 10 days at room temperature (0.451 g, 16%).

Method 2: Compound **4a** (see synthesis below) was oxidized using the method reported by Ronco and Erlenmeyer:[20] compound **4a** (10.00 g, 134.90 mmol) was dissolved in acetone (150 mL) and cooled to 0 °C. Solid potassium permanganate (14.47 g, 91.56 mmol) was then added slowly. A brown suspension was formed and the reaction mixture was allowed to warm to room temperature and stirred for 6 h. The insoluble manganese(IV) oxide was then removed by filtration through Celite and the volatile compounds of the resulting filtrate were removed under reduced pressure (50 °C). Crystals of the title compound separated crystallized out of the yellow solution upon cooling to room temperature. The yield was increased by storing the mother liquor in the fridge overnight (5.68 g, 51% based on compound **4a**).

^{1}H NMR ($CDCl_3$, 400.18 MHz, TMS): $\delta = 3.32$ (6H, s; CH_3), 8.94 ppm (2H, s; CHO); ^{13}C{^{1}H} NMR ($CDCl_3$, 100.52 MHz, TMS): $\delta = 27.11$ (1C; N−CH_3), 163.37 ppm (1C; CHO); ^{15}N NMR ($CDCl_3$, 40.51 MHz, NH_3): $\delta = +391.7$ (1N, s; N2), +193.2 ppm (1N, s, N1); DSC (5 °C min^{-1}): two endothermic peaks (peak 1: sharp, onset: 164.0 °C, maximum: 166.0 °C, peak 2: broad, onset: 194.8 °C, maximum: 197.2 °C), one exothermic peak (sharp, onset: 201.4 °C, maximum: 204.2 °C); GC: 23.52 min (acetone, method C[26]); GC-MS (ESI): *m*/*z* (%): 145.1 (5) $[M+H]^+$, 144.1 (97) $[M]^+$, 87.1 (3) $[M+H-N(CH_3)_2]^+$, 86.1 (7) $[M-N(CH_3)_2]^+$, 73.1 (20) $[HN{=}NN(CH_3)_2]$, 59.2 (31) $[HN(CH_3)(CHO)]^+$, 43.2 (100) $[CH_2{=}N(CH_3)]$, 48.2 (28) $[N_2]$, 15.2 (21) $[CH_3]^+$; Raman (rel. int.): $\tilde{\nu}$ = 3036(3), 2997(4), 2958(5), 2921(7), 2882(15), 1711(6), 1683(16), 1502(100), 1418(1), 1395(12), 1377(5), 1348(1), 1229(12), 1128(1), 1064(3), 1026(1), 904(4), 791(1), 418(9), 370(1), 321(3), 291 cm^{-1} (5); IR (golden gate, rel. int.): $\tilde{\nu}$ = 3035(w), 2996(w), 2955(w), 2918(w), 1756(w), 1665(m), 1647(m), 1467(m), 1445(w), 1410(w), 1400(w), 1390(w), 1338(s), 1272(w), 1226(m), 1128(w), 1087(w), 1031(s), 1021(s), 851(m), 668(m), 604(w), 573 cm^{-1} (s); elemental analysis calcd (%) for $C_4H_8N_4O_2$ (144.13): C 33.33, H 5.59, N 38.87; found: C 33.21, H 5.69, N 38.67.

*Synthesis of 1-Formyl-1-methylhydrazine (**4a**)*

The synthesis of **4a** was carried out according to a modified literature procedure:[23] 98% 1-methylhydrazine (10.5 mL, 9.187 g, 195.44 mmol) was dissolved in EtOH (15 mL) in a 100 mL round-bottomed flask. To this solution, 97% ethyl formate (16.0 mL, 14.672 g, 192.11 mmol) was added portionwise. A highly exothermic reaction took place and the reaction flask was immersed in an oil bath and heated to reflux for 6 h. After 6 h, the initial colorless solution had turned bright yellow and the solvent was removed under reduced pressure (50 °C). The yellow residue left in the flask was distilled using a 10 cm length cylinder-filled column under vacuum (10.692 g, 75%). ^{1}H NMR ([D$_6$]DMSO, 400.18 MHz, TMS): $\delta = 2.86$ (3H, s; CH_3), 4.11 (2H, br s; NH_2), 7.98 ppm (1H, s; CHO); ^{13}C NMR ([D$_6$]DMSO, 100.52 MHz, TMS): $\delta = 36.85$ (1C, s; CH_3), 164.32 ppm (1C, s; CHO); DSC (5 °C min^{-1}): > 170 °C (dec.), 199–200 (b.p.); GC: 20.08 min (EtOH, method C[26]); GC-MS (ESI): *m*/*z* (%): 75.2 (1) $[M+H]^+$, 74.2 (25) $[M]^+$, 59.2 (3) $[M-CH_3]^+$, 46.2 (86), 45.2 (100) $[M-CHO]^+$, 44.2 (12), 43.2 (17), 31.2 (24), 30.2 (30) $[M-CH_3-CHO]^+$, 29.2 (28) $[CHO]^+$, 28.2 (50) $[N_2]$, 18.1 (22) $[H_2O]$, 17.1 (4), 16.2 (2) $[NH_2]^+$, 15.2 (5) $[CH_3]^+$; Raman (rel. int.): $\tilde{\nu}$ = 3216(51), 3004(34), 2924-(100), 2792(14), 2553(3), 2393(2), 1675(24), 1416(62), 1312(15), 1236(11), 1082(14), 1013(8), 873(21), 849(61), 662(54), 607(3), 445(16), 421(15), 316 cm^{-1} (18); IR (golden gate, rel. int.): $\tilde{\nu}$ = 3446(w), 3315(w), 3213(w), 2924(w), 2882(w), 1652(s), 1484(w), 1418(w), 1398(w), 1359(m), 1234(m), 1081(m), 984(m), 871(m), 849(m), 662(m), 573(w), 563 cm^{-1} (w); elemental analysis calcd (%) for $C_2H_6N_2O$ (74.08): C 32.43, H 8.16, N 37.81; found: C 32.25, H 8.15, N 37.73.

Compound **4** was identified as the desired isomer, 1-formyl-1-methylhydrazine (**4a**), and not 1-formyl-2-methylhydrazine (**4b**), by formation of the corresponding acetone hydrazone by dissolving in dry acetone. GC: 20.78 (acetone, method A[26]), 16.06 min (acetone, method C[26]); GC-MS (ESI): *m*/*z* (%): 115.1 (2) $[M+H]^+$, 114.1 (23) $[M]^+$, 99.1 (100) $[M-CH_3]^+$, 85.2 (14) $[M-CHO]^+$, 71.2 (11), 56.1 (21) $[M-(CHO)CH_3]^+$, 42.2 (26) $[(CH_3)_2C]^+$, 30.2 (14) $[HC(=O)H]$, 29.1 (10) $[CHO]^+$, 28.2 (6) $[N_2]$, 15.2 (3) $[CH_3]^+$.

*Synthesis of 1-Formyl-2-methylhydrazine (**4b**)*

Compound **4b**, which was formed as a side-product during the synthesis of isomer **4a** (see above), was characterized by GC-MS and NMR spectroscopy from the reaction mixture without isolation. ^{1}H NMR ([D$_6$]DMSO, 400.18 MHz, TMS): $\delta = 2.90$ (3H, s; CH_3), 4.81 (2H, br s; NH), 7.73 ppm (1H, s; CHO); ^{13}C NMR ([D$_6$]DMSO, 100.52 MHz, TMS): $\delta = 35.20$ (1C, s; CH_3), 159.18 ppm (1C, s; CHO); GC: 18.17 min (MeOH, method C[40]); GC-MS (ESI): *m*/*z* (%): 75.2 (4) $[M+H]^+$, 74.2 (100) $[M]^+$, 59.2 (2) $[M-CH_3]^+$, 46.2 (41), 45.2 (62) $[M-CHO]^+$, 44.2 (8),

43.2 (11), 31.2 (20), 30.2 (9) [$M-CH_3-CHO]^+$, 29.2 (25) $[CHO]^+$, 28.2 (39) $[N_2]$, 18.1 (21) $[H_2O]$, 17.1 (3), 16.2 (2) $[NH_2]^+$, 15.2 (6) $[CH_3]^+$.

*Synthesis of Monoformylhydrazine (**8**)*

Hydrazine monohydrate (5.00 mL, 102.78 mmol) was dissolved in MeOH (30 mL) in a 100 mL round-bottomed flask before a solution of 97% ethyl formate (17.12 mL, 205.55 mmol) in MeOH (40 mL) was added dropwise, whilst the round-bottomed flask was cooled in a water bath. After the addition was finished, the water bath was warmed to 70 °C and the temperature was maintained for about 2 h. Then, the solvent was removed under reduced pressure to yield a white powder, which was dried under high vacuum and sublimed twice under high vacuum (50 °C) to give the pure title compound as colorless single crystals suitable for X-ray diffraction (4.906 g, 79%). ^{1}H NMR ([D$_6$]DMSO, 400.18 MHz, TMS): $\delta = 4.39$ (2H, s; NH_2), 7.90 (1H, s; CHO), 9.07 ppm (1H, s; NH); ^{13}C NMR ([D$_6$]DMSO, 100.52 MHz, TMS): $\delta = 160.23$ ppm (1C,;CHO); ^{15}N NMR ([D$_6$]DMSO, 40.51 MHz, NH_3): $\delta = +137.5$ (1N, s; NH(CHO)), +52.0 ppm (1N, s; NH_2); DSC (5 °C min^{-1}): two endothermic peaks (peak 1: sharp, onset: 57.2 °C, maximum: 65.0 °C; peak 2: broad, onset: ca. 150 °C, maximum: ca. 200 °C), one exothermic peak (broad, onset: ca. 220 °C, maximum: ca. 250 °C); GC: 22.20 min (MeOH, method C[26]); GC-MS (ESI): *m*/*z* (%): 61.1 (2) $[M+H]^+$, 60.1 (48) $[M]^+$, 45.1 (1) $[M-NH]^+$, 44.1 (3) $[M-NH_2]^+$, 43.1 (8) $[M-NH_3]^+$, 32.2 (100) $[N_2H_3+H]^+$, 31.2 (82) $[N_2H_3]^+$, 30.2 (12) $[CHO+H]^+$, 29.2 (53) $[CHO]^+$, 28.2 (10) $[CO]^+$, 17.1 (3) $[NH_2+H]^+$, 16.1 (5) $[NH_2]^+$, 15.1 (2) $[NH]^+$; Raman (rel. int.): $\tilde{\nu} = 3317(41)$, 3234(34), 3167(58), 3090(12), 2994(14), 2911(97), 2882(11), 2750(2), 1659(7), 1637(12), 1613(7), 1574(11), 1511(13), 1377(100), 1256(38), 1237(20), 1071(9), 1022(16), 982(37), 855(4), 803(9), 399(15), 353(12), 286(6), 202 cm^{-1} (49); IR (golden gate, rel. int.): $\tilde{\nu} = 3318$(w), 3159(m), 2990(w), 2906(w), 2749(w), 2035(w), 1666(m), 1626(m), 1506(m), 1378(w), 1254(m), 1195(w), 1039(m), 1022(m), 976(w), 787 cm^{-1} (s); elemental analysis calcd (%) for CH_4N_2O (60.05): C 20.00, H 6.71, N 46.65; found: C 19.87, H 6.59, N 46.42.

*Synthesis of 1,2-Diformylhydrazine (**9**)*

Hydrazine monohydrate (2.50 mL, 2.572 g, 51.39 mmol) was reacted with two equivalents of formamide (4.09 mL, 4.629 g, 102.78 mmol) in a 25 mL round-bottomed flask. The resulting solution was heated in a water bath (90 °C) for 2.5 h. The initial colorless solution turned pink and, by the end of the reaction, a pink solid had precipitated. Addition of EtOH (10 mL) resulted in the separation of a colorless powder, which was filtered, washed with EtOH and Et_2O and dried in air (2.690 g). Leaving the combined washings to stand overnight afforded the formation of single crystals of the compound (0.258 g). No further purification was necessary and both batches were combined (2.948 g, 65%). Similar results were obtained when ethyl formate or formic acid (according to the method reported by Liu et al.[23]) were used as the formylating agent: hydrazine monohydrate (2.00 mL, 2.058 g, 41.13 mmol) and 97% formic acid (3.52 mL, 4.292 g, 90.48 mmol) were reacted carefully in an ice bath and the resulting solution was heated to reflux for 5 h at 120 °C. After slow cooling to room temperature, single crystals of the title compound precipitated out of the solution, which were filtered, washed with cold water, acetone, and Et_2O (3.24 g, 89%). ^{1}H NMR ([D$_6$]DMSO, 400.18 MHz, TMS): $\delta = 9.96$ (2H, br s; NH), 8.01 ppm (2H, s; CHO); ^{13}C NMR ([D$_6$]DMSO, 100.52 MHz, TMS): $\delta = 159.05$ ppm (2C; CHO); ^{15}N NMR ([D$_6$]DMSO, 50.68 MHz, NH_3): $\delta = +130.5$ ppm (2N, dd, ^1J(N,H) = 21.8 Hz, ^2J(N,H) = 4.0 Hz;;HN–CHO); DSC (5 °C min^{-1}): 157.9 °C (m.p.); MS (–c ESI, H_2O): *m*/*z* (%): 59.0 (5) $[M-HCO]^-$, 87.1 (100) $[M-H]^-$, 99.0 (10), 122.9 (11) $[M+Cl]^-$; MS (+c ESI, H_2O): *m*/*z* (%): 89.0 (9) $[M+H]^+$, 111.0 (42) $[M+Na]^+$, 116.9 (52), 127.0 (15), 152.1 (100), 199.0 (35), 215 (43), 250.8 (28); Raman (rel. int.): $\tilde{\nu} = 3069(3)$, 2994(5), 2923(12), 2882(6), 1685(2), 1612(4), 1581(27), 1556(28), 1385(41), 1248(100), 1061(11), 1007(3), 863(7), 841(5), 460(16), 335(14), 296(17), 169 cm^{-1} (65); IR (golden gate, rel. int.): $\tilde{\nu} = 3107$(m), 2898(m), 2795(m), 2705(m), 2522(w), 2467(w), 2068(w), 1994(w), 1613(m), 1455(m), 1393(w), 1362(m), 1223(m), 993(w), 921(w), 826(w), 732(s), 720(s), 586(w), 578(w), 562 cm^{-1} (w); elemental analysis calcd(%) for $C_2H_4N_2O_2$ (88.06): C 27.28, H 4.58, N 31.81; found: C 27.12, H 4.48, N 31.56.

Acknowledgements

Financial support by the Centre National de la Recherche Scientifique (CNRS), the Centre National d'Études Spatiales (CNES), SAFRAN-SME and the University Claude Bernard of Lyon is gratefully acknowledged. The authors are also indebted to and would like to thank Dr. B. Fenet and Mr. S. Alamercery for performing the ^{15}N NMR and Raman spectroscopic measurements, respectively, and Dr. E. Jeanneau for performing the X-ray experiments and crystal-structure solution.

[1] a) T. M. Klapötke, C. Miró Sabaté, A. Penger, M. Rusan, J. M. Welch, *Eur. J. Inorg. Chem.* **2009**, 880–896; Sabaté, M. Rasp, *J. Mater. Chem.* **2009**, *19*, 2240–2252; Sabaté, *Z. Anorg. Allg. Chem.* **2007**, *633*, 2671–2677; b) T. M. Klapötke, C. Miró Sabaté, J. M. Welch, *Z. Anorg. Allg. Chem.* **2008**, *634*, 857–866; c) T. M. Klapötke, C. Miró Sabaté, *Chem. Mater.* **2008**, *20*, 3629–3637.

[2] a) K. Karaghiosoff, T. M. Klapötke, C. Miró Sabaté, *Chem. Eur. J.* **2009**, *15*, 1164–1176; b) M. Eberspächer, T. M. Klapötke, C. Miró Sabaté, *Helv. Chim. Acta* **2009**, *92*, 977–996; c) T. M. Klapötke, C. Miró Sabaté, M. Rasp, *J. Mater. Chem.* **2009**, *19*, 2240–2252; d) T. M. Klapötke, C. Miró Sabaté, *Z. Anorg. Allg. Chem.* **2010**, *636*, 163–175; e) H. Delalu, K. Karaghiosoff, T. M. Klapötke, C. Miró Sabaté, *Cent. Eur. J. Energ. Mater.* **2010**, *7*, 115–129.

[3] a) M. Göbel, T. M. Klapötke, *Z. Anorg. Allg. Chem.* **2007**, *633*, 1006–1017; b) G. Geisberger, T. M. Klapötke, J. Stierstorfer, *Eur. J. Inorg. Chem.* **2007**, 4743–4750; c) T. M. Klapötke, J. Stierstorfer, *Helv. Chim. Acta* **2007**, *90*, 2132–2150; d) J. Stierstorfer, T. M. Klapötke, A. Hammerl, R. D. Chapman, *Z. Anorg. Allg. Chem.* **2008**, *634*, 1051–1057; e) J. Stierstorfer, K. Tarantik, T. M. Klapötke, *Chem. Eur. J.* **2009**, *15*, 5775–5792; f) T. M. Klapötke, S. M. Sproll, *Eur. J. Org. Chem.* **2010**, 1169–1175; g) T. M. Klapötke, B. Krumm, R. Moll, *Eur. J. Inorg. Chem.* **2011**, 422–428.

[4] a) Y.-H. Joo, B. Twamley, S. Garg, J. M. Shreeve, *Angew. Chem.* **2008**, *120*, 6332–6335; *Angew. Chem. Int. Ed.* **2008**, *47*, 6236–6239; b) T. Abe, Y.-H. Joo, G.-H. Tao, J. M. Shreeve, *Chem. Eur. J.* **2009**, *15*, 4102–4110; c) G.-H. Tao, Y.-H. Joo, B. Twamley, J. M. Shreeve, *J. Mater. Chem.* **2009**, *19*, 5850–5854; d) Y.-H. Joo, J. M. Shreeve, *J. Am. Chem. Soc.* **2010**, *132*, 15081–15090; <*lit* e> Y. Huang, H. L. Gard, J. M. Shreeve, *Tetrahedron Lett.* **2010**, *51*, 6951–6954.

[5] H. Gao, Y.-H Joo, B. Twamley, J. M. Shreeve, *Angew. Chem.* **2009**, *121*, 2830–2833; *Angew. Chem. Int. Ed.* **2009**, *48*, 2792–2795.

[6] V. Forquet, C. Darwich, C. Miró Sabaté, H. Delalu, *Proceedings of the 13th New Trends in Research of Energetic Materials Seminar*, Pardubice, Czech Republic, **2010**.

[7] J. Heppekausen, T. M. Klapötke, S. M. Sproll, *J. Org. Chem.* **2009**, *74*, 2460–2466.

[8] T. M. Klapötke, N. K. Minar, J. Stierstorfer, *Polyhedron* **2009**, *28*, 13–26.

[9] T. M. Klapötke, P. Mayer A. Schulz, J. J. Weigand, *Propellants Explos. Pyrotech.* **2004**, *29*, 325.

[10] T. G. Back, *J. Chem. Soc. Chem. Commun.* **1981**, 530; D. H. Bae, H. J. Shine, *J. Org. Chem.* **1981**, *46*, 4700.

[11] a) N. Wiberg, H. Bayer, H. Bachhuber, *Angew. Chem.* **1975**, *87*, 202–203; b) N. Wiberg, H. W. Haering, S. K. Vasisht, *Z. Naturforsch. B* **1979**, *34*, 356–357.

[12] a) K. Karaghiosoff, T. M. Klapötke, P. Mayer, C. Miró Sabaté, A. Penger, J. M. Welch, *Inorg. Chem.* **2008**, *47*, 1007–1019; b) T. M. Klapötke, C. Miró Sabaté, A. Penger, M. Rusan, J. M. Welch, *Eur. J. Inorg. Chem.* **2009**, 880–896;.

[13] W. W. Schoeller, V. Staemmler, *Inorg. Chem.* **1984**, *23*, 3369–3373.

[14] F. O. Rice, C. J. Grelecki, *J. Am. Chem. Soc.* **1957**, *79*, 2679–2680.

[15] H. H. Sisler, M. A. Mathur, S. R. Jain, R. Greengard, *Ind. Eng. Chem. Prod. Res. Dev.* **1981**, *20*, 181–185.

[16] L. J. Madgzinski, K. S. Pillay, H. Richard, Y. L. Chow, *Can. J. Chem.* **1978**, *56*, 1657–1667.

[17] W. H. Urry, P. Szecsi, D. W. Moore, *J. Am. Chem. Soc.* **1964**, *86*, 2224–2229.

[18] S. N. Singh, R. K. Prasad, *J. Indian Chem. Soc.* **1992**, *69*, 648–650.

[19] a) W. E. Thun, W. R. McBride, *J. Org. Chem.* **1969**, *34*, 2997–3002; b) P. M. Gannett, C. Garrett, T. Lawson, B. Toth, *Fd. Chem. Toxic.* **1991**, *29*, 49–56.
[20] K. Ronco, H. Erlenmeyer, *Helv. Chim. Acta* **1956**, *39*, 1045–1051.
[21] R. L. Hinman, D. Fulton, *J. Am. Chem. Soc.* **1958**, *80*, 1895.
[22] C. T. Pedersen, *Acta Chem. Scand.* **1964**, *18*, 2199–2000.
[23] A. Liu, T. Fang, X. Zhenyou, Q. Xiao, L. Zhang, *Wuhan Gongcheng Daxue Xuebao* **2008**, *30*, 28–30.
[24] T. M. Klapötke, C. Miró Sabaté, *New J. Chem.* **2009**, *33*, 1605–1617.
[25] N. B. Colthup, L. H. Daly, S. E. Wiberley in *Introduction to Infrared, Raman Spectroscopy*, Academic Press, Boston, USA, **1990**.
[26] Method A: maintain temperature at 45 °C for 1 min, then heat at 4 °C min^{-1} to 130 °C; method B: maintain temperature at 45 °C for 1 min, then heat at 6 °C min^{-1} to 150 °C; method C: maintain temperature at 45 °C for 1 min, then heat at 6 °C min^{-1} to 230 °C.
[27] R. G. Parr, W. Yang, *Density Functional Theory of Atoms, Molecules*, Oxford University Press, New York, USA, **1989**.
[28] a) M. C. Etter, J. C. MacDonald, *Acta Crystallogr. Sect. B* **1990**, *46*, 256–262; b) J. Bernstein, R. E. Davis, L. Shimoni, N. L. Chang, *Angew. Chem.* **1995**, *107*, 1689–1708; *Angew. Chem. Int. Ed. Engl.* **1995**, *34*, 1555–1573;.
[29] These data can be obtained free of charge from The Cambridge Crystallographic Data Centre via www.ccdc.cam.ac.uk/data_request/cif.
[30] A. F. Hollemann, E. Wieberg, N. Wieberg in *Lehrbuch der Anorganische Chemie*, *101th ed.*, Walter de Gruyter, Berlin, Germany, **1995**.
[31] C. Darwich, T. M. Klapötke, C. Miró Sabaté, *Propellants Explos. Pyrotech.* **2008**, *33*, 336–346.
[32] a) H. Hope, T. Ottersen, *Acta Crystallogr. Sect. B* **1979**, *35*, 370–372; b) H. Hope, T. Ottersen, *Acta Crystallogr. Sect. B* **1978**, *34*, 3623–3626; c) Y. Tomiie, C. H. Koo, I. Nitta, *Acta Crystallogr.* **1958**, *11*, 774–781.
[33] H. Brand, A. Schulz, K. Polborn, private communication, **2005**, CCDC 279587.
[34] M. D. Harmony, V. W. Laurie, R. L. Kuczkowski, R. H. Schwedeman, D. A. Ramsay, F. L. Lovas, W. J. Lafferty, A. G. Maki, *J. Phys. Chem. Ref. Data* **1979**, *8*, 619–721.
[35] C. Darwich, T. M. Klapötke, C. Miró Sabaté, *Chem. Eur. J.* **2008**, *14*, 5756–5771.
[36] http://www.bam.de.
[37] http://www.reichel-partner.de.
[38] *UN Recommendations on the Transport of Dangerous Goods*: Impact: Insensitive > 40 J, less sensitive ≥ 35 J, sensitive ≥ 4, very sensitive ≤ 3 J. Friction: Insensitive > 360 N, less sensitive = 360 N, sensitive < 360 N and > 80 N, very sensitive ≤ 80 N, extremely sensitive ≤ 10 N.
[39] a) *NATO standardization agreement (STANAG) on explosives, impact sensitivity tests*, no. 4489, Ed. 1, Sept. 17, **1999**; b) *NATO standardization agreement (STANAG) on explosive, friction sensitivity tests*, no. 4487, Ed. 1, Aug. 22, **2002**.
[40] a) *WIWEB-Standardarbeitsanweisung 4–5.1.02, Ermittlung der Explosionsgefährlichkeit, hier der Schlagempfindlichkeit mit dem Fallhammer*, Nov. 8, **2002**; b) *WIWEB-Standardarbeitsanweisung 4–5.1.03, Ermittlung der Explosionsgefährlichkeit oder der Reibeempfindlichkeit mit dem Reibeapparat*, Nov. 8, **2002**.
[41] J. Köhler, R. Meyer in *Explosivstoffe*, *9th ed.*, Wiley-VCH, Weinheim, Germany, **1998**.

Received: September 12, 2011
Published online: January 20, 2012

